Drug Repositioning for Scorpion Envenomation Treatment Through Dual Inhibition of Chlorotoxin and Leiurotoxin

Bioinformatics and Biology Insights
Volume 18: 1–9

DOI: 10.1177/11779322241294130

Gaouzi Zainab[1,2#], Abbou Hanane[1,2#], Zegrari Razana[1,2], Eljaoudi Rachid[1,3], Diawara Idrissa[1,2], Hakmi Mohammed[1] and Mkamel Mouad[1]

[1]Mohammed VI Center for Research and Innovation, Rabat, Morocco. [2]Mohammed VI University of Sciences and Health, Casablanca, Morocco. [3]Biotechnology Lab (MedBiotech), Bioinova Research Center, Medical and Pharmacy School, Mohammed V University in Rabat, Rabat, Morocco.

#These authors contributed equally to this work and share first authorship

Diawara Idrissa is now affiliated to Mohammed VI University of Sciences and Health, Mohammed VI Higher Institute of Biosciences and Biotechnologies (UM6SS), Casablanca, Morocco.

Gaouzi Zainab, Abbou Hanane, Zegrari Razana, Eljaoudi Rachid, Eljaoudi Rachid, Mkamel Mouad are now affiliated to Mohammed VI University of Sciences and Health (UM6SS), Morocco.

Eljaoudi Rachid, Hakmi Mohammed, Mkamel Mouad are now affiliated to Mohammed VI Center for Research and Innovation (CM6RI), Morocco.

ABSTRACT: Scorpion envenomation, a grave public health concern, is primarily driven by the potent neurotoxins chlorotoxin and leiurotoxin present in Leiurus species venom. Developing effective treatments is crucial to mitigate its impact. Utilizing a drug-repositioning bioinformatics-based approach, potential inhibitors of these neurotoxins were identified from Food and Drug Administration (FDA)-approved drugs. Through virtual screening and subsequent molecular dynamics simulations, their ability to stabilize the peptides over time was evaluated. Among the compounds scrutinized, bolazine emerged as a promising candidate, demonstrating significant affinity for both neurotoxins, indicating potential dual inhibitory activity. Molecular dynamics simulations further corroborated the enhanced stability of bolazine complexes compared to neurotoxins alone. These findings suggest the feasibility of repurposing existing drugs to develop new therapeutic strategies to treat scorpion envenomation. Such interventions hold promise in alleviating the severe health repercussions of scorpion stings and meeting the urgent demand for effective remedies in affected communities.

KEYWORDS: Scorpion venom, chlorotoxin, leiurotoxin, inhibitors, drug repositioning

RECEIVED: May 18, 2024. **ACCEPTED:** October 8, 2024.

TYPE: Research Article

FUNDING: The author(s) received no financial support for the research, authorship, and/or publication of this article.

DECLARATION OF CONFLICTING INTERESTS: The author(s) declared no potential conflicts of interest with respect to the research, authorship, and/or publication of this article.

CORRESPONDING AUTHOR: Gaouzi Zainab, Mohammed VI University of Sciences and Health, Boulevard Mohammed taïeb Naciri, Commune Hay Hassani 82 403, Zip code :20100, Casablanca, Morocco. Email: zgaouzi@um6ss.ma

Introduction

Scorpion envenomation poses a significant threat to public health,[1] particularly in regions where venomous species such as the *Leiurus scorpion*, commonly known as the Deathstalker, are prevalent. This species, predominantly found in North Africa and the Middle East,[2] has garnered notoriety for its potent venom, which harbors a complex mixture of toxins capable of inducing severe symptoms in humans, including muscle spasms, respiratory distress, and cardiovascular complications,[3] necessitating immediate medical intervention to counteract the venom's effects.[4,5]

Among these toxins, neurotoxins such as chlorotoxin (CTX) and leiurotoxin (ScyTx), are notably potent, disrupting normal nerve signaling by binding to ion channels and causing severe effects such as pain, paralysis, and potentially fatal outcomes if untreated.[3] The CTX specifically binds to chloride (Cl^-) ion channels,[6] whereas ScyTx binds to calcium (Ca^{2+})-dependent potassium (K^+) channels.[7,8] On injection into the body, these neurotoxins rapidly diffuse throughout the bloodstream, targeting specific ion channels and receptors on nerve cells, thereby interfering with neurotransmitter function.[9,10]

In light of the imperative demand for efficacious therapeutic strategies to address scorpion envenomation, drug repositioning has emerged as a promising strategy. This approach involves repurposing existing drugs for new therapeutic applications,[11] potentially accelerating the drug discovery process by bypassing lengthy preclinical testing phases.[12] By leveraging computational approaches such as virtual screening, molecular docking, and molecular dynamics (MD) simulations, researchers can systematically evaluate large databases of approved drugs to identify potential candidates.[13] This innovative approach not only expedites the identification of potential treatments,[14] but also offers the possibility of uncovering unexpected therapeutic candidates that may have been overlooked in traditional drug development pipelines.[15]

In this study, we will exploit drug-repositioning principles, through a pathogenic toxin-based neutralizing drug approach.

Focusing on the two neurotoxins CTX and ScyTx, we will attempt to identify potential neutralizing drugs using computational methods.

Methods

Structures' retrieval and preparation for docking

The three-dimensional (3D) structures of the peptides CTX and ScyTx were obtained from the Protein Data Bank (PDB IDs: 7X43 and 1SCY, respectively). Notably, PDB 7X43 had a mutation at the first amino acid (R), which was corrected to the wild-type methionine (M) using the Maestro module. After this correction, the structures were refined using the protein preparation wizard in the Schrödinger suite.[16] This process involved the removal of water molecules and heteroatoms, as well as the addition of missing hydrogen atoms to ensure structural completeness. Finally, the prepared structures were visualized with PyMol to explore their conformational features.

High throughput virtual screening

High throughput virtual screening (HTVS) of Food and Drug Administration (FDA)-approved drugs library (4574 molecules) against the prepared PDB structures of the peptides using the online server MTiOpenScreen[17] (https://bioserv.rpbs.univ-paris-diderot.fr/services/MTiOpenScreen/). It is based on Vina docking algorithms and provides five electronic chemical libraries, among which is the drug library used in our study. The screening focused on identifying ligands with favorable binding affinities to each peptide (CTX and ScyTx). The results of the HTVS were ranked based on the binding energy of their best scoring conformation. The top five best-interacting molecules for each peptide were selected, and the molecule in both selections was further studied. The docking results for the chosen molecule were visualized using Pymol,[18] and the ligand interaction diagram was generated using LigPlot+.[19]

Molecular dynamics simulation

The molecule that showed a high binding affinity with both peptides was selected for MD simulations. The resulting structures from the docking process and the prepared PDBs of the peptides were used as the starting conformation for the simulations after an initial step of preparation conducted using the system builder wizard in Desmond.[20] The preparation consisted of embedding the CTX–bolazine complex, ScyTx–bolazine complex, CTX and ScyTx in a simple point charge (SPC) solvent using a Cubic box system with 10 Å padding, neutralizing the systems, then adding 0.15 M of sodium chloride (NaCl).

The generated systems were then subjected to 100 ns MD simulations using OPLS4 force field, with a recording step of 100 ps, in an NPT ensemble class, under 300 K temperature and 1.01325 bar pressure using the MD module in Desmond.[20]

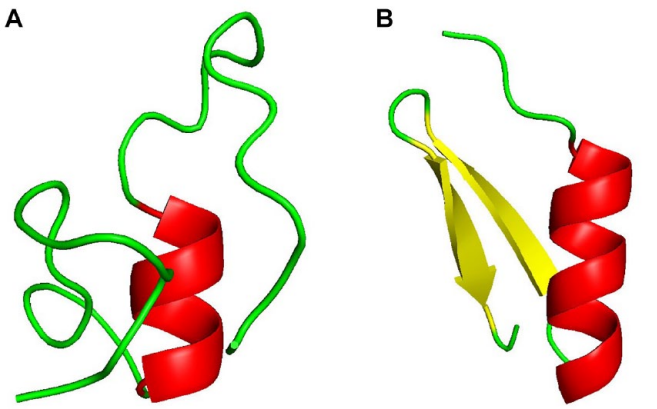

Figure 1. Three-dimensional (3D) structures of toxins. (A) Chlorotoxin (PDB: 7X43). (B) Leiurotoxin (PDB: 1SCY), where red regions indicate alpha helix, yellow regions indicate beta sheet, and green regions indicate unrestrained residues of the peptides.

After completing the MD simulation of each system, the resulting trajectories were analyzed using the Simulation Interaction Diagram (SID) implemented in Maestro to quantify the system's dynamics using the root mean square deviation (RMSD), root mean square fluctuation (RMSF), the radius of gyration (Rg), and solvent accessible surface area (SASA). The average (Avg) and standard deviation (SD) for each parameter were calculated, and protein secondary structure elements (SSE), such as alpha-helices and beta-strands, were monitored throughout the simulation of each residue.

Results and Discussion

Structure preparation

The 3D structures of the peptides CTX and ScyTX (see Figure 1). After structural preparation and refinement, the corrected models displayed a well-preserved architecture, with all missing hydrogen atoms appropriately added and extraneous components removed.

Molecular docking

Molecular docking is a computational technique used in structural biology and drug discovery. It has become a key tool for identifying molecules with potential binding affinity for a given receptor. It provides insights into the binding mechanisms and interactions between ligands and receptors, which aids in the drug discovery process.[21]

Following the structural refinement of CTX and ScyTx, the top five ligands from the HTVS output were selected based on their favorable docking scores (see Tables 1 and 2). For ScyTx, these ligands exhibited docking scores ranging from −7.3 kcal/mol to −8 kcal/mol, while for CTX, the scores ranged from −7.2 kcal/mol to −7.9 kcal/mol, indicative of strong binding affinities. The top five molecules for each neurotoxin were analyzed and the interactions were visualized (see Figures S1 and

Table 1. Docking scores of the top five FDA-approved drugs selected for chlorotoxin.

COMPOUND	BINDING ENERGY, KCAL/MOL
R428_ZINC000051951669	–7.9
Bolazine_ZINC000008214506	–7.7
Golvatinib_ZINC000043195317	–7.2
Nilotinib_ZINC000006716957	–7.2
R428_ZINC000051951668	–7.2

Table 2. Docking scores of the top five FDA-approved drugs selected for leiurotoxin.

COMPOUND	BINDING ENERGY, KCAL/MOL
Bolazine_ZINC000008214506	–8
R428_ZINC000051951668	–7.5
R428_ZINC000051951669	–7.5
Mk3207_ZINC000103760984	–7.4
Proscillaridin_ZINC000306121903	–7.3

S2). Remarkably, among the top-scoring ligands, two compounds, bolazine and bemcentinib (R428_ZINC000051951669), were common between the two sets. Not only were they common among the highest-scoring binding ligands, but they also demonstrated consistent performance: bolazine displayed the highest docking score of –8 kcal/mol with ScyTx and the second highest score of –7.7 kcal/mol with CTX, while bemcentinib exhibited the highest score of –7.9 kcal/mol with CTX and the third highest score of –7.5 kcal/mol with ScyTx. While comparing bolazine and bemcentinib (R428_ZINC000051951669) for CTX, bemcentinib had a better score, but bolazine had more interactions with additional amino acids (AA; see Figure S1A and B). For ScyTx, both ligands interacted with the same number of AA; however, bolazine formed an additional hydrogen bonds (HBs) with Arg13 (see Figure S2A and C) and had a higher docking score. On comprehensive analysis, it was observed that bemcentinib is currently undergoing clinical trials for anti-tumor treatment.[22] In contrast, bolazine has been previously commercialized as an anabolic steroid, suggesting an established safety profile and potential utility in therapeutic applications.[23] Therefore, bolazine was prioritized over bemcentinib for further investigation. Bolazine's proven safety profile, drug-likeness, and commercial availability make it a promising candidate for drug-repositioning targeting CTX and ScyTx.

Molecular interactions between bolazine and the neurotoxins

Bolazine, also known as 2α,17α-dimethyl-5α-androstan-17β-ol-3-one azine,[24] is a synthetic androgen/anabolic steroid (AAS).[25] AAS such as bolazine are synthetic compounds derived from testosterone, a natural hormone produced in the body.[26] They are widely used in the medical field to treat conditions such as delayed puberty in adolescents and hormonal disorders.[27]

In our study, we evaluated the docking scores of CTX with bolazine, yielding a high score of –7.7 kcal/mol (see Table 1). This significant score suggests an optimal interaction between multiple AA and our selected ligand. Notably, our docking results further revealed hydrophobic interactions between the ligand and several cysteine residues including Cys5, Cys16, Cys28, and Cys33 (see Figure 2), where it has been established that disulfide bonds between CTX's cysteins (Cys) Cys2–Cys19, Cys5–Cys28, Cys16–Cys33, and Cys20–Cys35 are essential for its structural integrity and stability.[28,29] This observation hints at the potential of bolazine to disrupt two intra-peptide interactions, by preventing the formation of two disulfide bonds, consequently compromising the overall functional structure of CTX.

Similarly, ScyTx–bolazine docking score is –8 kcal/mol (see Table 2), with diverse interactions, encompassing hydrophobic interactions and an HB. Previous research has shown the role of arginine residues (Arg6 and Arg13) in ScyTx's binding to the Ca^{2}+-activated K^{+} channel protein, mediating its toxic effects.[30] Our ligand interaction diagram (see Figure 3) confirms the specific binding of bolazine to ScyTx through Arg6 and Arg13. This finding suggests the potential for our ligand to interfere with peptide interactions with the ion channel, thereby impeding its toxic activity.

Molecular dynamics analysis

The MD simulation is a powerful computational tool for studying the movements of complex macromolecular systems, including biomolecules. It enhances molecular docking models by considering the flexibility of proteins and ligands, leading to a more accurate representation of the binding process and the identification of more effective drug candidates.[31]

An important aspect of MD simulations is the analysis of the structural fluctuations of the macromolecule. It can be used to identify key conformational changes that occur on ligand binding and subsequently provide insights into the molecular basis of ligand–target interactions.[32]

Chlorotoxin. The MD simulation results show a clear difference in structural fluctuation between CTX and CTX–bolazine over time. The RMSD analysis is a reliable metric for studying protein structural changes over time; the lower the average RMSD value, the more stable the structure.[33] The lower its average value, the more stable the structure is.

The RMSD values of CTX alone (Avg = 0.90, SD = 0.20) are significantly lower than those of CTX–bolazine complex (Avg = 2.34, SD = 0.36; see Table 3), suggesting that bolazine's interaction with the peptide induces internal motion in the peptide and subsequently conformational changes (see Figure 4A).

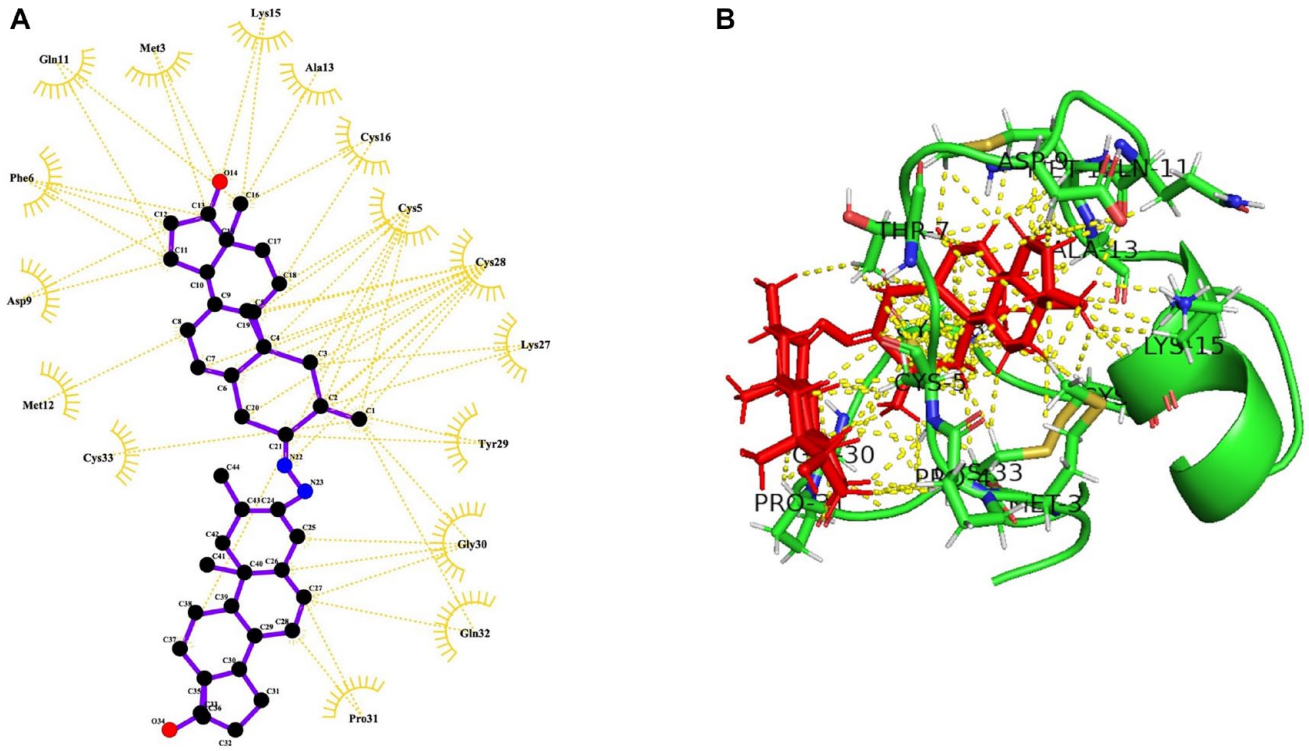

Figure 2. The CTX–bolazine complex interaction and binding interface. (A) Two-dimensional (2D) structure of complex interactions. (B) Three-dimensional (3D) visualization of complex interactions. The CTX peptide is represented in green, bolazine molecule in red. Hydrophobic interaction regions within the complex are outlined in yellow.

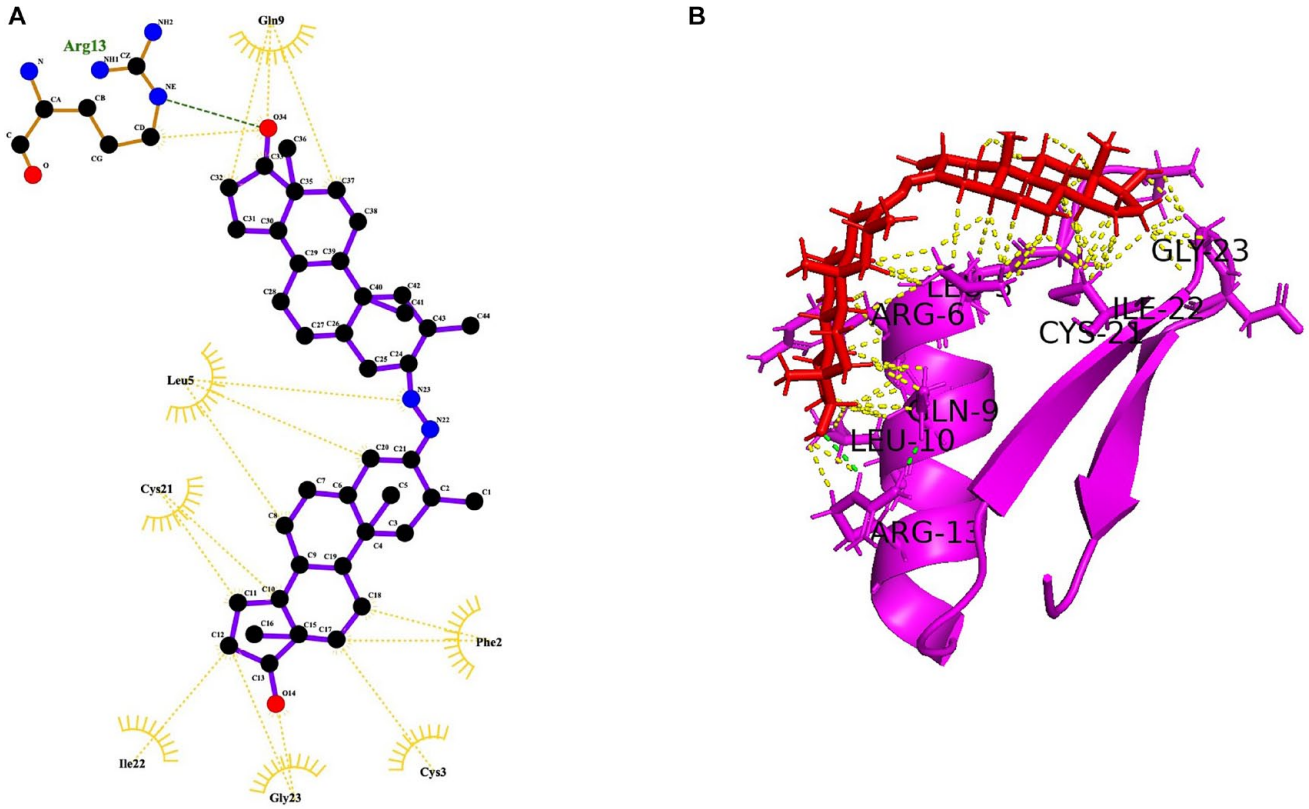

Figure 3. The ScyTx–bolazine complex interaction and binding interface. (A) Two-dimensional (2D) structure of complex interactions. (B) Three-dimensional (3D) visualization of complex interactions. The ScyTx peptide is illustrated in magenta, while the bolazine molecule is depicted in red. Hydrophobic interaction regions within the complex are outlined in yellow and H-bond interaction regions in green.

Table 3. The averges and standard deviations of the parameters generated from molecular dynamics of the four 3D structures.

PARAMETERS	ANALYZED STRUCTURES							
	CTX		CTX–BOLAZINE		SCYTX		SCYTX–BOLAZINE	
	AVG	SD	AVG	SD	AVG	SD	AVG	SD
RMSD	0.90	0.20	2.34	0.36	1.35	0.26	1.56	0.31
RMSF	0.61	0.25	0.95	0.45	0.86	0.57	0.87	0.63
Rg	21.90	0.04	21.97	0.04	0.86	0.05	0.87	0.04
SASA	4084.80	91.83	4431.46	99.19	4038.12	104.73	4603.25	165.57

Abbreviations: Avg, average; CTX, chlorotoxin; ScyTx, leiurotoxin; Rg, radius of gyration; RMSD, root mean square deviation; RMSF, root mean square fluctuation; SASA, solvent accessible surface area.

This fluctuation is apparent through RMSF, an important parameter that reflects the structural flexibility of Cα atoms of each residue in its corresponding system.[34] The majority of the AA in the CTX–bolazine complex (Avg = 0.96, SD = 0.45) show significantly higher values compared to the AA in the CTX alone (Avg = 0.61, SD = 0.25; see Table 3).

Concurring with the docking results, Cys5, Cys16, Cys28, and Cys33 are all in interaction with the ligand, demonstrated by higher RMSF values per residue (see Figure 4B), which according to our data, induced higher fluctuation and so potentially interfered with the creation of disulfide bonds within the neurotoxin, especially between Cys5 and Cys28, as these two residues spent the highest faction of simulation time in interaction with Balozine (see Figure S3). The peptide's instability, attributed to its inability to form internal disulfide bonds, hindered its ability to attain the necessary functional conformation. During the simulation, HBs between CTX and bolazine were observed, fluctuating between 0 and 2 HBs over the course of the simulation period (see Figure S4).

The Rg as an indicator of biomolecule structure compactness.[35] The higher the Rg value, the less compact the structure is. The Rg of CTX–bolazine (Avg = 21.97, SD = 0.04) is higher than Rg of CTX (Avg = 21.90, SD = 0.04; see Table 3 and Figure 4C), meaning that bolazine reduced the compactness of CTX, which further proves the reduced number of intramolecular interactions.

Another interesting parameter is the SASA of a molecule, which refers to the portion of its surface that can interact with the surrounding solvent.[36] This parameter helps assess the compactness of the studied molecule. The value for SASA of the CTX–bolazine complex is (Avg = 4431.46, SD = 99.19), whereas the SASA value for CTX alone is (Avg = 4048.80, SD = 91.83). The larger surface area indicates that the peptide has lost its initial compact structure due to its interaction with bolazine (see Figure 4D).

On visual analysis of the final frame from the MD simulation and SSE monitoring, we found that Arg14 lost its helical secondary structure. Throughout the simulation, we notice considerable conformational changes in multiple residues, such as Cys33 and Leu34, which went from forming a loop to adopting a beta-sheet conformation repeatedly through the first 60 ns of the simulation time. Moreover, Arg14, which maintained its helix structure for the first 40 ns, started alternating between a loop and helix form until the end of the simulation where it adopted the loop conformation (see Figures 6A and S5).

The combination of the previously discussed parameters demonstrates bolazine's potential to cause significant internal motion in CTX, altering its functional structure. This prevents it from binding to chlorine ion channels and exerting its toxic effect.

Leirotoxin. The RMSD values observed for the ScyTx alone (Avg = 1.35, SD = 0.26) are notably lower compared to those of the ScyTx–bolazine complex (Avg = 1.56, SD = 0.31; see Table 3), indicating that bolazine's interaction induces internal motion and subsequent conformational changes in the peptide (see Figure 5A). This fluctuation is further evidenced by the RMSF analysis, where the majority of AA in the ScyTx–bolazine complex (Avg = 0.87, SD = 0.63) exhibit higher values compared to those in ScyTx alone (Avg = 0.86, SD = 0.57; see Table 3 and Figure 5B).

Both Arg6 and Arg13, which are needed for ScyTx binding to the Ca^{2+} activated K^{+} channels, interact with the ligand, which probably induces the variation of the respective RMSF values[30] (see Figure S6). This interaction would prevent the formation of bonds with ion channels, rendering the neurotoxin incapable of fulfilling its biological function. The docking results revealed that Arg13 formed one HB with bolazine, then throughout the simulation, the number of HBs fluctuated between 0 and 3, with 1 being the most frequently observed (see Figure S4b).

Moreover, the Rg of the ScyTx–bolazine complex (Avg = 22.43, SD = 0.04) is higher than that of ScyTx alone

Figure 4. Plots of structural fluctuations of CTX alone (red) and CTX–bolazine complexes (green) over 100 ns molecular dynamics simulation. (A) The RMSD values in Angstroms (Å) over simulation time. (B) The RMSF values in Angstroms (Å) along the residue positions. (C) The Rg values in Angstroms (Å) through the simulation time (ns). (D) The SASA values respectively, in Angstroms (Å) through the simulation time (ns).

(Avg = 21.96, SD = 0.05; see Table 3), indicating a reduced compactness attributed to fewer intramolecular interactions (see Figure 5C).

Similarly, the SASA value for the ScyTx–bolazine complex (Avg = 4603.25, SD = 165.57) is higher than that of ScyTx alone (Avg = 4038.12 SD = 104.73; see Table 3), suggesting a loss of initial compact structure due to interaction with bolazine (see Figure 5D).

The SSE monitoring and final frame structure analysis demonstrate that Cys21 and Lys25 have lost their secondary structure, which is a beta-sheet. The Cys21 started losing its structure and morphed into a loop in the first few nanoseconds, then regained a beta-sheet structure for multiple time lapses during the simulation, before the final step in the simulation where it adopted the loop secondary structure. Similarly, for Lys25, an almost identical structural fluctuation profile to that of Cys21 was observed, indicating that some residues struggle to keep their secondary structure in the presence of bolazine (see Figures 6B and S7).

These findings collectively underscore bolazine's potential to prevent ScyTx from binding to the ion channel exerting its toxic effects.

Bolazine, a potential dual inhibitor

Bolazine's binding to the two neurotoxins altered their biological function through different mechanisms, suggesting a dual inhibitory potential. It caused significant changes in CTX's secondary structures and internal peptide motion by interacting with residues crucial for structural stability, such as Cys. As for ScyTx, the drug-induced conformational changes were less damaging than those caused for CTX, still, they were impactful and noticeable as previously demonstrated through the multiple MD simulation results. The inhibition mechanism which is

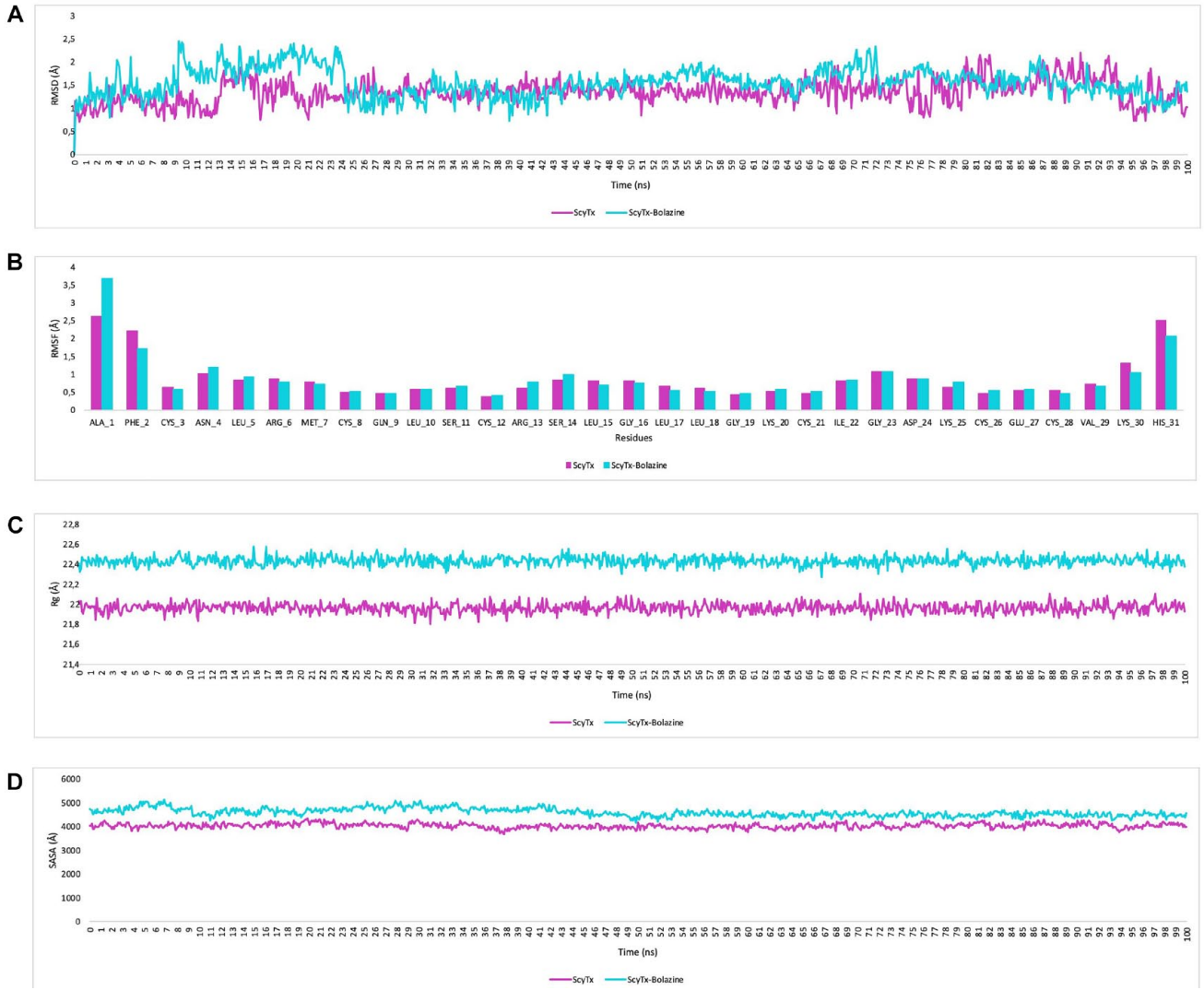

Figure 5. Plot depicting the structural dynamics of ScyTx alone (magenta) and the ScyTx–bolazine complex (cyber blue) throughout a 100 ns molecular dynamics simulation. (A) The RMSD values in Angstroms (Å) over simulation time. (B) The RMSF values in Angstroms (Å) along the residue positions. (C) The Rg values in Angstroms (Å) through the simulation time (ns). (D) The SASA values, respectively, in Angstroms (Å) through the simulation time (ns).

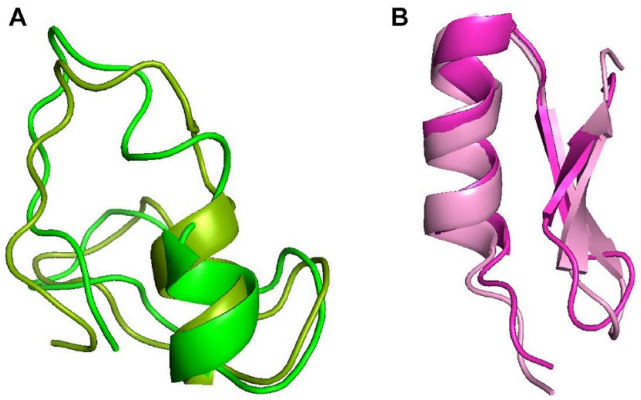

Figure 6. Superposition of first and last frames of: (A) CTX–bolazine with the ligand omitted and (B) ScyTx–bolazine with ligand omitted.

supposedly the one that will alter the biological function of ScyTx is the binding to important residues for the interaction with the target human ion channels.

Bolazine's promising inhibitory mechanism becomes more intriguing when the presence of CTX-like peptides in multiple scorpion species is added to the equation. A sequence alignment of different CTX-like peptides illustrates that the sequence is generally well conserved across species, with the segments between the 1st to 9th residue and the 30th to 35th residue being the most conserved.[37] Our MD simulation of the CTX–bolazine showed that the drug is capable of forming strong bonds lasting for considerable fractions of the simulation time, hinting at the possibility of repositioning bolazine against multiple CTX-like peptides, and thereby, potentially neutralizing the venoms of multiple scorpion species.

Neurotoxins found in scorpion venom, such as CTX and ScyTx, represent a serious threat due to their ability to disrupt nerve signal transmission, resulting in a spectrum of debilitating symptoms, including muscle weakness, paralysis, autonomic dysfunction, and central nervous system disturbances. Moreover, severe envenomation can lead to respiratory distress, cardiovascular complications, and seizures.[38] Current reliance on antivenoms, while life-saving, is hindered by limitations such as limited availability, variable effectiveness across snake species, and high costs.[39] In this context, the proposal of bolazine, through a drug-repositioning strategy, as a dual inhibitor presents a promising alternative. Bolazine's small molecule nature and pharmacological properties offer advantages in terms of tissue distribution and efficacy in mitigating peripheral tissue damage commonly seen in scorpion bite envenoming. By providing a therapeutic bridge until antivenoms are accessible, bolazine-based interventions have the potential to significantly improve patient outcomes and address the critical need for more effective treatments against the morbidity caused by scorpion envenomation.

Despite the promising initial findings, rigorous validation through further *in vitro* studies is essential to ensure that bolazine can effectively address the diverse range of scorpion venom compositions and the varying severity of envenomation cases.

Conclusions

The imperative demand for efficacious remedies to address scorpion envenomation remains a major public health concern. We leveraged the drug-repositioning strategy to identify a potential FDA-approved molecule as an emergency treatment to alleviate the scorpion envenoming burden on the affected communities. Further *in vitro* testing would be beneficial to further validate the potential of bolazine as a scorpion venom neutralizer.

Author Contributions

GZ and AH were involved in the conceptualization, investigation, software, visualization and writing of the original draft. ZR contributed to methodology writing of the original draft and writing – review and editing. EJR and DI were involved in the supervision and validation. MH contributed toward critical review and final article editing. MM was involved in the data curation, supervision, and validation.

ORCID iD

Gaouzi Zainab https://orcid.org/0009-0008-9167-5228

SUPPLEMENTAL MATERIAL

Supplemental material for this article is available online.

REFERENCES

1. Forde A, Jacobsen A, Dugon MM, Healy K. Scorpion species with smaller body sizes and narrower chelae have the highest venom potency. *Toxins*. 2022;14:219.
2. Alqahtani AR, Badry A. Genetic diversity among different species of the genus Leiurus (Scorpiones: Buthidae) in Saudi Arabia and the Middle East. *Saudi J Biol Sci*. 2020;27:3348-3353.
3. Amr ZS, Abu Baker MA, Al-Saraireh M, Warrell DA. Scorpions and scorpion sting envenoming (scorpionism) in the Arab Countries of the Middle East. *Toxicon*. 2021;191:83-103.
4. Soulaymani Bencheikh R, Idrissi M, Tamim O, et al. Scorpion stings in one province of Morocco: epidemiological, clinical and prognosis aspects. *J Venom Anim Toxins Incl Trop Dis*. 2007;13:462-471.
5. Chakroun-Walha O, Karray R, Jerbi M, et al. Update on the epidemiology of scorpion envenomation in the South of Tunisia. *Wilderness Environ Med*. 2018;29:29-35.
6. DeBin JA, Maggio JE, Strichartz GR. Purification and characterization of chlorotoxin, a chloride channel ligand from the venom of the scorpion. *Am J Physiol*. 1993;264:C361-C369.
7. *Leiurus quinquestriatus* venom inhibits different kinds of Ca2+-dependent K+ channels. Accessed April 5, 2024. https://www.sciencedirect.com/science/article/abs/pii/0005273686900544
8. Moczydlowski E, Lucchesi K, Ravindran A. An emerging pharmacology of peptide toxins targeted against potassium channels. *J Membr Biol*. 1988;105:95-111.
9. Ali SA, Stoeva S, Schütz J, et al. Purification and primary structure of low molecular mass peptides from scorpion (*Buthus sindicus*) venom. *Comp Biochem Physiol A Mol Integr Physiol*. 1998;121:323-332.
10. Joseph B, George J. Scorpion toxins and its applications. *Int J Toxicol Pharmacol Res*. 2012;4:57-61.
11. Talevi A, Bellera CL. Challenges and opportunities with drug repurposing: finding strategies to find alternative uses of therapeutics. *Expert Opin Drug Discov*. 2020;15:397-401.
12. Krishnamurthy N, Grimshaw AA, Axson SA, Choe SH, Miller JE. Drug repurposing: a systematic review on root causes, barriers and facilitators. *BMC Health Serv Res*. 2022;22:970.
13. Parvatikar PP, Patil S, Khaparkhuntikar K, et al. Artificial intelligence: machine learning approach for screening large database and drug discovery. *Antiviral Res*. 2023;220:105740.
14. Ng YL, Salim CK, Chu JJH. Drug repurposing for COVID-19: approaches, challenges and promising candidates. *Pharmacol Ther*. 2021;228:107930.
15. Parvathaneni V, Kulkarni NS, Muth A, Gupta V. Drug repurposing: a promising tool to accelerate the drug discovery process. *Drug Discov Today*. 2019;24:2076-2085.
16. *Schrödinger Release 2021-2: Maestro*. Schrödinger, LLC, 2021.
17. MTiOpenScreen: a web server for structure-based virtual screening. *Nucleic Acids Res*. Accessed April 4, 2024. https://academic.oup.com/nar/article/43/W1/W448/2467861
18. Schrödinger LLC. The PyMOL molecular graphics system, version 1.8. Published 2015. https://pymol.org/support.html
19. Laskowski RA, Swindells MB. LigPlot+: multiple ligand–protein interaction diagrams for drug discovery. *J Chem Inf Model*. 2011;51:2778-2786.
20. Schrödinger release 2021-2: Desmond molecular dynamics system, D. E. Shaw Research, 2021. Maestro-Desmond Interoperability Tools, Schrödinger, 2021.
21. Pinzi L, Rastelli G. Molecular docking: shifting paradigms in drug discovery. *Int J Mol Sci*. 2019;20:4331.
22. Bhalla S, Fattah FJ, Ahn C, et al. Phase 1 trial of bemcentinib (BGB324), a first-in-class, selective AXL inhibitor, with docetaxel in patients with previously treated advanced non-small cell lung cancer. *Lung Cancer*. 2023;182:107291.
23. Khanna V, Ranganathan S. Physicochemical property space distribution among human metabolites, drugs and toxins. *BMC Bioinformatics*. 2009;10:S10.
24. National Center for Biotechnology Information. PubChem compound summary for CID 20055426, Bolazine. Published 2024. Accessed April 4, 2024. https://pubchem.ncbi.nlm.nih.gov/compound/Bolazine
25. Rogozkin VA. *Metabolism of Anabolic-Androgenic Steroids*. CRC Press; 1991.
26. van Amsterdam J, Opperhuizen A, Hartgens F. Adverse health effects of anabolic–androgenic steroids. *Regul Toxicol Pharmacol*. 2010;57:117-123.
27. Albano GD, Amico F, Cocimano G, et al. Adverse effects of anabolic-androgenic steroids: a literature review. *Healthcare*. 2021;9:97.
28. Ojeda PG, Chan LY, Poth AG, Wang CK, Craik DJ. The role of disulfide bonds in structure and activity of chlorotoxin. *Future Med Chem*. 2014;6:1617-1628.

29. Meng X, Xu C, Fan S, et al. Selection and evolution of disulfide-rich peptides via cellular protein quality control. *Chem Sci*. 2023;14:3668-3675.
30. Auguste P, Hugues M, Mourre C, Moinier D, Tartar A, Lazdunski M. Scyllatoxin, a blocker of Ca(2+)-activated K+ channels: structure-function relationships and brain localization of the binding sites. *Biochemistry*. 1992;31:648-654.
31. Shukla R, Tripathi T. Molecular dynamics simulation of protein and protein-ligand complexes. In: Singh, DB, ed. *Computer-Aided Drug Design*. Springer; 2020:133-161.
32. Karplus M, McCammon JA. Molecular dynamics simulations of biomolecules. *Nat Struct Biol*. 2002;9:646-652.
33. Pitera JW. Expected distributions of root-mean-square positional deviations in proteins. *J Phys Chem B*. 2014;118:6526-6530.
34. Ul Haq F, Abro A, Raza S, Liedl KR, Azam SS. Molecular dynamics simulation studies of novel β-lactamase inhibitor. *J Mol Graph Model*. 2017;74:143-152.
35. Lobanov MYu, Bogatyreva NS, Galzitskaya OV. Radius of gyration as an indicator of protein structure compactness. *Mol Biol*. 2008;42:623-628.
36. Durham E, Dorr B, Woetzel N, Staritzbichler R, Meiler J. Solvent accessible surface area approximations for rapid and accurate protein structure prediction. *J Mol Model*. 2009;15:1093-1108.
37. Ojeda PG, Wang CK, Craik DJ. Chlorotoxin: structure, activity, and potential uses in cancer therapy. *Biopolymers*. 2016;106:25-36.
38. Del Brutto OH. Neurological effects of venomous bites and stings. In: *Handbook of Clinical Neurology*. Elsevier; 2013:349-368. Accessed April 8, 2024. https://linkinghub.elsevier.com/retrieve/pii/B9780444534903000285